

Plasma dynamic synthesis of ultradispersed zinc oxide and sintering ceramics on its basis by SPS method

Yu Shanenkova, A Sivkov, A Ivashutenko, I Shanenkov and K Firsov
National Research Tomsk Polytechnic University, 30 Lenin av., Tomsk, 634050,
Russia

E-mail: julia_kolganova@mail.ru

Abstract. Zinc oxide is a well-known semiconductor material having good electrical, optical and catalytic properties. It can be used in different areas from cosmetics to drug delivery and biosensors. The synthesis of nanosized zinc oxide is an urgent task for obtaining ZnO-based ceramics with enhanced physical properties. This work shows the possibility to implement the plasma dynamic synthesis of zinc oxide in one short-term process (less than 1 ms) using an electrodischarge zinc-containing plasma jet, flowing into oxygen atmosphere. It allows synthesizing a mono-crystalline powder with particle size distribution from tens to hundred nanometers. The synthesized powdered product is investigated using by X-Ray diffractometry (XRD), scanning electron microscopy and high-resolution transmission electron microscopy. According to XRD, the obtained product consists of hexagonal zinc oxide with lattice parameters $a = b = 3.24982 \text{ \AA}$, $c = 5.20661 \text{ \AA}$ that is clearly confirmed by microscopy data. This powder was used to produce a bulk ceramics sample on its basis by spark plasma sintering. The influence of sintering parameters on the structure of the resulting sample was studied. The optimal parameters were found which allows obtaining the more dense ceramics with a better microstructure. It was also found that the absence of exposure time after reaching the working temperature and pressure allows decreasing the porosity of ceramics.

1. Introduction

It is well known that zinc oxide is a promising material because of its properties such as high electron mobility, good transparency, wide bandgap, strong luminescence [1]. In addition, the last studies of this material have allowed opening good catalytic properties of ZnO [2-7]. All of these unique characteristics make zinc oxide useful for using in different production areas such as nanobiology, nanomedicine, piezoelectric generators, optoelectronic and photovoltaic devices [8-13].

The properties of zinc oxide strongly depend on its structure, morphology, aspect ratio, size and orientation of the particles [14-16]. ZnO crystallites with the different particle morphology, for example, spherical, prism, stars, rods and others, have been previously studied [17-23]. Nonetheless, the hexagonal structure of zinc oxide is of great scientific interest [24, 25].

Except the material structure, the particle size is also an important factor for ZnO. Nanodispersed powders are widely used in science and technology because of their unique properties (low density and high specific surface features) [26]. In spite of this, in some scientific areas it has a special interest in obtaining a particular particle forms with a wide distribution from several tens to hundreds of nanometers [27]. For example, in order to create a high density ceramic, it is necessary to introduce particles of smaller fraction (nanoparticles) in a micron or submicron powder [28].



This paper shows a unique method for obtaining nanodispersed zinc oxide using a system based on a coaxial magneto plasma accelerator. The main advantages of this method are the high speed of the process, as well as the high purity of the synthesized product, which has the desired structure and particle size distribution. This work reports the plasma dynamic synthesis that allows obtaining ultradispersed zinc oxide in the one short cycle (up to 10^{-3}) of CMPA work. Using XRD and HRTEM it is found that the synthesized product consists of single-crystalline hexagonal ZnO particles with the necessary stoichiometry. The particle size distribution histogram allows affirming that the product has the broad distribution up to 350 nm. It is also shown that the synthesized product can be used for sintering bulk samples using Spark Plasma Sintering (SPS) technology. The density of the obtained ceramics sample is up to 99%.

2. Experimental

The previous article [29] showed a scheme and the operation principle of coaxial magnetoplasma accelerator with zinc electrodes [30,31]. Using this accelerator, the nanodispersed ZnO powder was synthesized. After collecting the product of a plasma-dynamic synthesis, it was studied by means of X-ray diffractometry (XRD), scanning electron microscopy (SEM) and transmission electron microscopy (TEM) methods. After that, this product was sintered, using the setup for spark plasma sintering (Advanced Technology SPS 10-4).

Scanning electron microscopy (SEM) images were recorded using a Hitachi TM-3000 scanning microscope with carbon substrate. X-Ray diffraction (XRD) analysis was carried out using a Shimadzu XRD 7000S diffractometer (CuK α -radiation) with the counter monochromator Shimadzu CM 3121. The database PDF-2 and the software PowderCell 2.4 were used to make full-profile structural analysis and estimative calculations. Transmission electron microscopy (TEM) images of the product were made using a Philips CM-12 microscope. The particle size distribution histogram was built by measuring the size of several hundred particles in accordance with data of a number of bright-field TEM images. High resolution transmission electron microscopy (HRTEM) was carried out using a Jeol JSM-7500FA microscope.

3. Results and discussion

It was experimentally found that almost pure crystalline zinc oxide ZnO in the considered system is formed when the volume oxygen (O₂) concentration in a gas mixture is over than 80%. This is confirmed by the XRD pattern of the initial product (fig. 1). Its analysis showed the closeness of the synthesized powder to the structural model of ZnO of the hexagonal crystal system (space group P6₃mc (no.186)) with the lattice parameters $a=b=3.24982 \text{ \AA}$, $c=5.20661 \text{ \AA}$ (card number 36-1451) [32]. A full-profile structural analysis allowed estimating the average value of the coherent-scattering regions (CSR) for the crystalline phase ZnO, which was equal to $\sim 124.0 \text{ nm}$, as well as the average level of internal microscopic strains in the crystal structure ($\Delta d/d=0.043 \cdot 10^{-3}$). The last parameter indicates the weakly strained state of the single-crystalline particle structure in the synthesized powder. It is also a reason for a good agreement between the calculated values of the lattice parameters $a=b=3.24970 \text{ \AA}$, $c=5.20270 \text{ \AA}$ with the previously mentioned parameters, which are closest to the structural model of the zinc oxide. Such a structure for even nanoscale ZnO particles became evident after analyzing the data of transmission electron microscopy (fig. 2a). The high density of ZnO particle ($\rho = 5.61 \text{ g/cm}^3$) allowed obtaining high-quality brightfield and darkfield TEM images.

An analysis of SEM and TEM images showed that the particles had a broad enough size distribution from 10 nm to 500 nm. However, in order to get the more detailed information on the size of the particles, the distribution of the particle size was calculated, using a number of bright-field TEM-images, and the corresponding histogram was built (figure 2b). It is possible to see that particles have a wide size distribution up to 350 nm. The reason for this is the pulsed nature of the plasma-dynamic processes, during which the formed plasma flew out from the accelerator channel in free space. The regulation of plasma parameters at this stage seems to be not possible. At the end of the process, when the energy parameters of plasma and its temperature decrease, the cooling rate drops

sharply that leads to an increase in particle size. Nonetheless, about 85% of ZnO particles have sizes not more than 150 nm that is in a good agreement with the average value of CSR (XRD data).

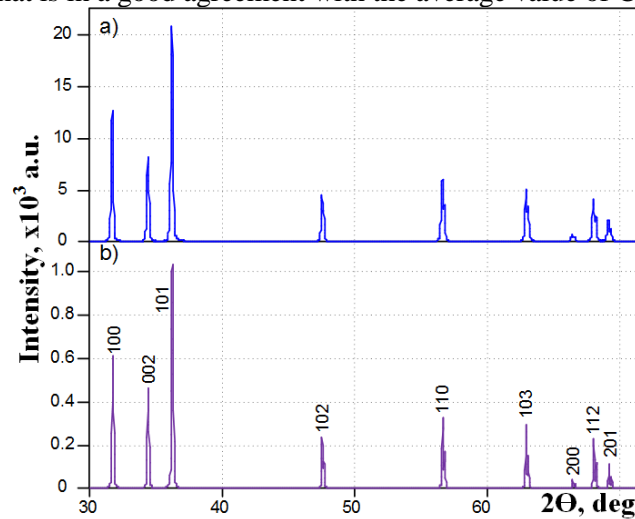


Figure 1. Typical XRD patterns a) for product of plasma dynamic synthesis in Zn-O system; b) structural model of hexagonal zinc oxide.

Judging by TEM images, the single-crystalline particles have an almost perfect crystallographic design in the form of hexagonal rods, as it is shown in the inset of figure 2. Regardless of the overall crystallite sizes, in this and similar clusters there are the particles, the length of which is either greater than the width of the lateral faces or less. The comparison of bright-field and dark-field images in the light of diffracted beams (corresponding reflexes are pointed by the Miller indices) shows a full compliance of reflecting plane systems to the theoretical model.

The marked features of the particle size distribution and the size ratio of their facets are connected with the pulse nature of the plasma-dynamic synthesis process. A very wide range of current change (from 0 up to 100 kA) provides the same wide range of changes of pressure and temperature (from room to approximately 10^4 K) in the discharge plasma, as well as the plasma jet velocity and velocity of spraying the liquid phase of the synthesized material in the chamber space. This influences the material crystallization rate, the size and shape of the crystallites. A detailed analysis of these processes requires additional special studies and is not the subject of this work.

It is known that for obtaining the high-quality ceramics with the micron and submicron structure by spark plasma sintering (SPS) it is necessary to introduce the finer fraction in quantity of 45 % in the main micron or submicron powder. In plasma-dynamic synthesis powders, this condition is automatically satisfied because of a uniform distribution the nanodispersed fraction in the total mass. While the powder is being compacted, the fine fraction fills the space between the larger particles, providing obtaining the high-density ceramics.

Due to the absence of the experience, the first experiments on the SPS-compaction of ultrafine ZnO powders were carried out in the mode, the main parameters of which were determined according to the published data [26]. The powder was compacted without any preliminary preparation in a vacuum. A graphite mold and punches with a diameter of 20 mm were used. A heating unipolar pulse current was switched on after compressing the dispersed sample between the punches with a pressure of 60 MPa. The temperature was raised stepwise with a rate of 50 °C/min to 600 °C, then at a rate of 10 °C/min to 800 °C. After reaching the preset maximum temperature, the temperature lowering was carried out at a rate of 50 °C/min to the room temperature. Only after the moment, when the temperature became equal to the room temperature, the pressure was removed from the sample.

The material density, measured by the hydrostatic method, was equal to $\rho = 4.5$ g/cm³ (80%), that indicates its high porosity. The SEM-images of the chip (figure 3) show the high heterogeneity of the

bulk material structure (fig. 3a). Its main mass has a nanoporous structure, formed by the ZnO particle-crystallites, which are united by crosspieces, which can be formed during spark sintering (fig. 2). In the sintered material, there are larger rounded particles, which are present in the original powder too.

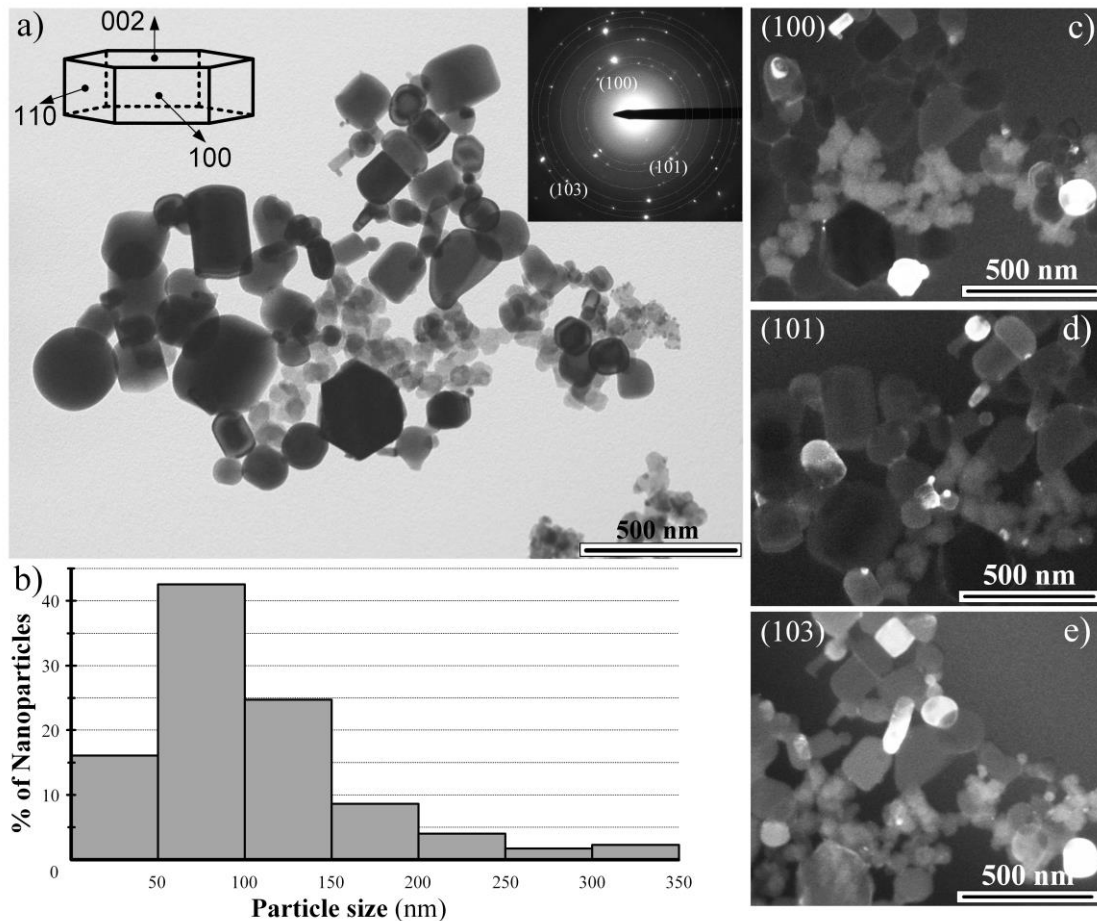


Figure 2. a) TEM data for initial product of plasma dynamic synthesis, consisting of single-crystalline particles of zinc oxide; b) histogram of powder particle size c)-e) dark-field images in the light of diffracted beams.

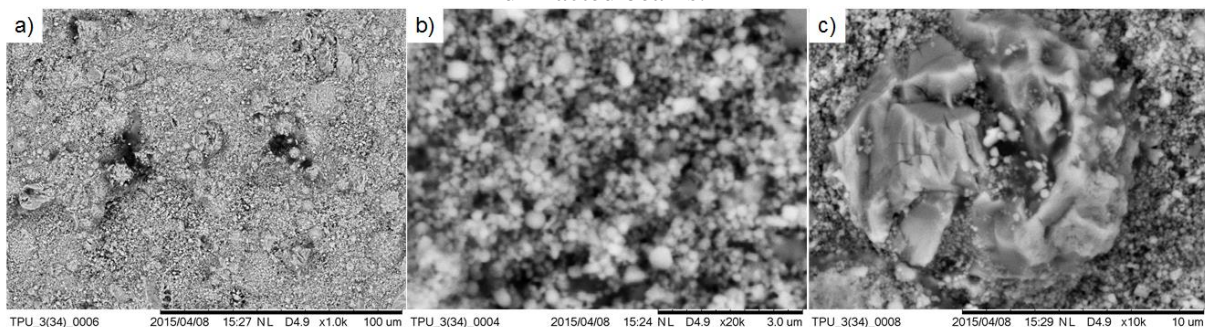


Figure 3. SEM-images of surface chip of ceramics sample: a) x1.0k, b) x20.0k, c) x10.0k.

In the sintered material, an obvious inhomogeneity is created by numerous focal defects of the rounded shape, with sizes up to several tens of microns and a typical coarse-grained structure (fig. 3b). This structure is formed by densely packed monolithic grains with sizes up to $\sim 5.0 \mu\text{m}$. These features indicate a liquid-phase mechanism of the formation of point defects. Such particles, having such sizes

and shapes, do not exist in the initial ZnO powder (figure 3). However, the dense agglomerates of nanoscale particles have even larger sizes. These dense agglomerates may be the reason for forming point defects during SPS-compaction, because there can be a local increase in both the density of the heating current and the realized energy. This leads to the melting of nanoparticles and the formation of large rounded focal points of the liquid ZnO phase. The melt crystallization with the formation of close-packed micron-sized grains occurs, when the heating current and cooling of the pressing are reduced.

Analysis of the results of the first experiments on the SPS-compaction showed the necessity to disaggregate powders and to optimize the heating mode. In this regard, before the next experiment, the product of the plasma-dynamic synthesis was subjected to the heat treatment in air at 200 °C for 1 hour with the followed processing in a ball mill (corundum crucible and a ball) at 30 minutes. The SPS process was also carried out in a graphite mold at a constant pressure of 50 MPa.

In the presented experiment, the heating mode was substantially changed. The speed of temperature growth was ~ 800 °C/min with the maximum level of 1100 °C. The process was carried out without isothermal exposure and with the natural cooling of the sample under pressure. As a result, the sample of ZnO-ceramics had the high density $\rho = 5.6$ g/cm³ (99.9%) that influenced its high thermal conductivity ($\lambda = 32.0$ W/m·K). Studies of ceramics sample by scanning electron microscopy (SEM) showed the absence of focal macro defects (figure 4) that should be considered as a positive result of disaggregating the initial ZnO powder.

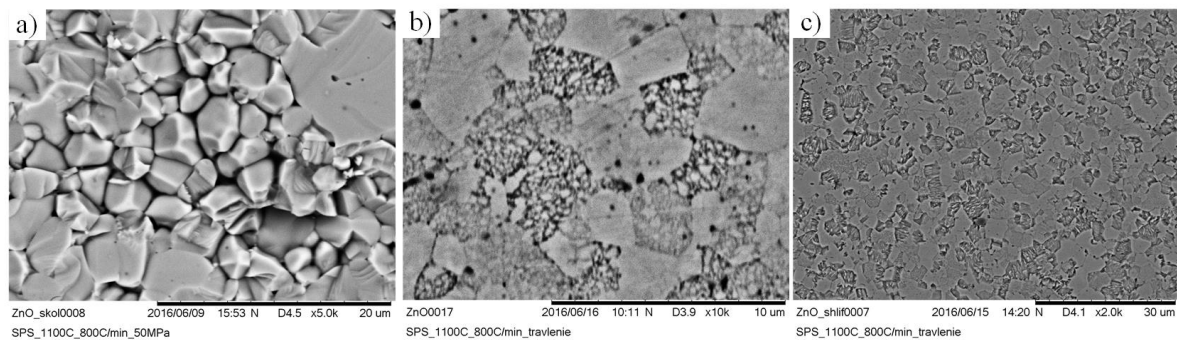


Figure 4. SEM-images of microstructure of obtained SPS-ceramics:

a) transverse chip of sample b) etching surface for 1 second c) etching surface for 30 seconds.

The transverse chip of the sample (figure 4a) passes through the volume of grains that indicates the strength of grain boundaries. The sizes of the largest grains do not exceed ~ 5.0 μm . Numerically insignificant large (open) pores with size up to ~ 1.0 μm were generally formed because of a non-completion of the triple grain boundaries. In addition, in the bodies of some large grains, there are small (less than 0.5 microns) closed pores. In the SEM-image, it is seen that surfaces of the chip of the smaller part of the grains have a layered nature, which seems to be caused by internal substructure of the grains.

Figure 4b shows an image of the sample flat surface, which is normal to the pressing direction, after a short etching for 1.0 seconds in a 5 percent solution of glacial acetic acid at different magnifications. The image is made in the mode of detecting back scattered electrons (COMPO), which gives the contrast in density of the material. It is seen that a large part of the surface cross-section (75%) consists of cuts of dense grains with a relatively light contrast. A smaller part of the surface area consists of grains, the cut surfaces of which were subjected to severe etching, which provided the development of the internal substructure. It is formed by particles, which consist of the densest material and give the brightest contrast.

The longer etching of the cross-section for 30 seconds does not lead to an increase in the total area of the material etching. However, it shows (fig. 4c) that strongly etched grains of ZnO ceramics microstructure consist of parallel micron-sized crystals with needle shape, which is a characteristic for zinc oxide of the hexagonal crystal structure. In addition, SEM-image seeing the substructure of the

dense grain, which is almost impervious to strong etching. This and similar SEM-images show the cuts (in the plane of cross-section) of elongated ZnO nanocrystals, Z-axis of which in the crystallographic direction (002) (figure 2a) nearly coincide with the pressing direction.

4. Conclusion

Thus, using a system based on a coaxial magnetoplasma accelerator and an installation for the spark plasma sintering, a bulk sample of SPS-ceramics based on hexagonal ZnO with the monocrystalline structure was obtained. The studies of its microstructure allow concluding that the obtained ceramics is quite dense with no visible focal defects. Such a structure of the sample is provided by the fact that the synthesized product of plasma-dynamic synthesis contains both nanoscale and micron size particles which is a positive moment for creating the ceramics.

Reference

- [1] Duong T T, Do Q N, Pham A T and Nguyen D C 2016 *J. Alloys Compd.* **686** 854-858
- [2] Yan H Q, He R R, Yang P D 2003 *J. Pham, Adv. Mater.* **15(5)** 402-405
- [3] Pourmortazavi S M, et al. 2015 *J. Molec. Struct.* **1099** 232-238
- [4] Lanje A, et al. 2013 *Adv. Powder Technol.* **24** 331-335
- [5] Lu P, Huang S, Chen Y, Chiueh L, Shih D 2015 *J. Food Drug Anal.* **23** 587-594
- [6] Zarrinkhameh M, Zendehnam A, Hosseini S M 2015 *J. Ind. Eng. Chem.* **30** 295-301
- [7] Sedláč J, et al. T 2015 *Adv. Powder Technol.* **26** 1064-1071
- [8] Moezzi A, McDonagh A M, Cortie M B 2012 *Chem. Eng. J.* **185** 1-22
- [9] Roy D, Fendler J. 2004 *Adv. Mater.* **16(6)** 479-508
- [10] Law M, Greene L, Johnson J, Saykally R and Yang P. 2005 *Nature materials* **4(6)** 455-459
- [11] Vanmaekelbergh D, Van Vugt L K 2011 *Nanoscale* **3(7)** 2783-2800
- [12] Liu Z, Song H, Yu L and Yang L 2005 *Appl. Phys. Lett.* **86(11)** 3109
- [13] Zhao M H, Wang Z L and Mao S X 2004 *Nano Lett.* **4(4)** 587-590
- [14] Hong R, Li J, Chen L, Liu D, Li H, Zheng Y and Ding J 2009 *Powder Technol.* **189(3)** 426-432
- [15] Wang H et al. 2013 *Adv. Powder Technol.* **24(3)** 599-604
- [16] Jagadish C and Pearton S J 2011 *Zinc oxide bulk, thin films and nanostructures: processing, properties, and applications* (Elsevier)
- [17] Dao V D, Choi Y, Yong K, Larina L L and Choi H S 2015 *Carbon* **84** 383-389
- [18] Liu X, et al. 2009 *J. Am. Chem. Soc.* **131(42)** 15106-15107
- [19] Zhang J, Zhao B, Pan Z, Gu M, Punnoose A 2015 *Cryst. Growth Des.* **15(7)** 3144-3149
- [20] Xu S, Li Z H, Wang Q, Cao L J, He T M and Zou G T 2008 *J. Alloys Compd.* **465(1)** 56-60
- [21] Jitianu M and Goia D V 2007 *J. Colloid Interface Sci.* **309(1)** 78-85
- [22] Anand V and Srivastava V C 2015 *J. Alloys Comp.* **636** 288-292
- [23] Xu S, Li Z H, Wang Q, Cao L J, He T M and Zou G T 2008 *J. Alloys Comp.* **465(1)** 56-60
- [24] Wang V, Ma D, Jia W and Ji W 2012 *Solid State Commun.* **152(22)** 2045-2048
- [25] Topsakal M, Cahangirov S, Bekaroglu E and Ciraci S 2009 *Phys. Rev. B* **80(23)** 235119
- [26] Rahimi-Nasrabadi M, et al. M 2015 *J. Mol. Struct.* **1083** 229-235
- [27] Simonelli G, Arancibia E L 2015 *J. Molec. Liquids* **211** 742-746
- [28] Xu Z et al. 2016 *Ceram. Int.* **42(13)** 14350-14354
- [29] Sivkov A, et al. 2016 *Adv. Powder Technol.* **27(4)** 1506-1513
- [30] Sivkov A, Saigash, A and Kolganova Y 2013 *Russian Electrical Engineering* **84(8)** 418-421
- [31] Kuzenov V V, Polozova T N, Ryzhkov S V 2015 *Problems of Atomic Science and Technology* **4** 98
- [32] Sivkov A, Shanenkova Y, Saigash A and Shanenkov I 2016 *Surf. Coat. Technol.* **292** 63-71
- [33] Damonte L C, et al. 2004 *Powder Tech.* **148** 15-19

Acknowledgements

This work was supported by the Russian Science Foundation (grant № 15-19-00049).